Available online at www.sciencedirect.com
SCIENCE DIRECT®
PERGAMON
Polyhedron 22 (2003) 2175–2181
POLYHEDRON
www.elsevier.com/locate/poly

New nickel dithiolene–diselenolene complexes obtained from 3,4-dichloro-1,2,5-thiadiazole X-ray structure of $(Bu_4N)_2[Ni(C_2N_2S_{2.2}Se_{0.8})_2]$

Paola Deplano [a,*], Luciano Marchiò [b], Maria Laura Mercuri [a], Luca Pilia [a], Angela Serpe [a], Emanuele F. Trogu [a]

[a] *Dipartimento di Chimica Inorganica ed Analitica, Università di Cagliari, Cittadella di Monserrato, I-09042 Monserrato, Cagliari, Italy*
[b] *Dipartimento di Chimica Generale ed Inorganica, Chimica Analitica, Chimica Fisica, Università di Parma, Parco Area delle Scienze 17A, I-43100 Parma, Italy*

Received 7 October 2002; accepted 10 February 2003

Abstract

The new $(Bu_4N)_2[Ni(C_2N_2S_{2.2}Se_{0.8})_2]$ (**1**) redox active nickel complex with a mixed $S_{0.6}/Se_{0.4}$ occupancy of thiolic sulfurs in the 1,2,5-thiadiazole-3,4-dithiolate (tdas) ligand has been prepared by reacting in situ $NiCl_2 \cdot 6H_2O$ with the products of the selenation reaction (grey selenium with $NaBH_4$ in EtOH) of 3,4-dichloro-1,2,5-thiadiazole ($TDACl_2$). Single crystal X-ray analysis of **1** shows that in the dianion, the central Ni-atom exhibits a square-planar geometry and that bond distances and angles are in agreement with those usually found in this class of complexes, except for the C–C distance [1.428(5) Å] which is longer than those generally found in dianionic metal dithiolene or diselenolene complexes. The position at unusually low frequency (1311 cm^{-1}) of the C=C stretching vibration in the Raman spectra agrees with structural results. A cyclic voltammetric study on **1** shows that the introduction of the selenium atom in the dithiolene core has the effect to make the dianion more easily to be oxidised than the corresponding tdas derivative. By chemical oxidation with I_2, $Bu_4N[Ni(C_2N_2S_{2.2}Se_{0.8})_2]$ (**2**) has been obtained. The existence of a monoanion as isolated species in solution and as dimers strongly antiferromagnetically coupled in the solid state is inferred from spectroscopic and EPR results.

Keywords: Ni dithiolenes; Se-donors; Raman; X-ray; Electrochemistry

1. Introduction

Interest in metal bis-dithiolene complexes is due to their wide application in the area of molecular materials showing electro-conducting [1], magnetic [2] and optical properties [3]. By virtue of the delocalised nature of these complexes, reversible redox processes are generally observed and mono- and di-anions can be obtained. Moreover the capability of these complexes to further extend the delocalisation of the dithiolene core by introducing atoms which can also mediate intermolecular interactions, the possibility that they can be diamagnetic or paramagnetic depending on the metal, gives the possibility to use them as counterions of suitable donors, potential carriers of electro-conducting properties. This can lead to materials showing multiproperties, such as molecular metals having magnetic or optical properties where an interplay or a co-existence of the functionalities of the two components may be found. Nickel complexes of the ligand 1,2,5-thiadiazole-3,4-dithiolate (tdas) [4] were proposed as potential analogs of the dmit complexes (dmit = 1,3-dithiole-2-thione-4,5-dithiolate), the unique class of complexes showing so far superconductivity [1]. However, the electro-conducting properties of the $(TTF)_2[Ni(tdas)_2]$ salt (TTF = tetrathiafulvalene) seemed unrewarding (room conductivity 1.0×10^{-1} S cm^{-1}) [4a], when compared with $(TTF)[Ni(dmit)_2]$ which exhibits superconductivity under pressure [5]. Instead, the iron salt $Bu_4N[Fe(tdas)_2]$

* Corresponding author. Tel.: +39-70-6754680; fax: +39-70-6754456.
E-mail address: deplano@vaxca1.unica.it (P. Deplano).

0277-5387/03/$ - see front matter © 2003 Elsevier Science Ltd. All rights reserved.
doi:10.1016/S0277-5387(03)00189-X

[6], which exhibits a dimeric structure and a magnetic behaviour typical of an antiferromagnetic dimer, shows interesting magnetic properties with two unusual phase transitions in the 190–240 K range, explained as a re-entrant phase behaviour where the low and high temperature phases are identical while a different phase exists between them. A TTF salt of the $[Fe(tdas)_2]$ anion has been prepared and characterised: $(TTF)_2[Fe(tdas)_2]$ [7] is a semiconductor and exhibits thermally activated magnetic behaviour. Recently the crystal structure of $(OMTTF)_2[Ni(tdas)_2]$ (OMTTF = octamethylenetetrathiafulvalene), which is an insulator consisting of a dimer of the radical cations and the $[Ni(tdas)_2]$ dianion, has been reported [8]. Attempts to prepare crystals of new CT salts of other donors, including ET, with $[Ni(tdas)_2]$ anions gave unsatisfactory results, and the reasons for this failure were not explained. The redox properties of nickel–tdas complexes have been reinvestigated and show, differently to what previously reported [4a], the presence of a two-step redox process for the $[Ni(tdas)_2]$ dianion's oxidation [8]. Moreover, the nature of the tdas ligand has been discussed in order to show the capability of the terminal sulfur atoms to promote intermolecular interactions [8]. These results prompted further investigations and after many attempts, crystals suitable for a structural characterisation of $(ET)_2[Fe(tdas)_2]$ [9] and $(BETS)_2[Fe(tdas)_2]_2$ [10] have been obtained by electrocrystallisation methods. Both salts show conducting and magnetic properties; the ET derivative has a semiconducting behaviour while the BETS salt a metallic character down to 200 K. The extended sulfur framework of ET compared with the TTF molecule allows for increased side-to-side sulfur–sulfur interactions in the $(ET)_2[Fe(tdas)_2]$ salt leading to improved electrical conductivity (room conductivity 3×10^{-2} and 1 S cm^{-1}, respectively). The substitution of four of the eight sulfur atoms of ET with selenium in BETS favours the metallic state due to increased polarisabilities and orbital overlap between molecules induced by Se-atoms. With the view to investigate the influence of the substitution of the Se-atoms also in tdas-based counterions of the above cited cations, we have attempted the selenation reaction of the 3,4-dichloro-1,2,5-thiadiazole ($TDACl_2$) molecule, obtaining in the presence of the nickel chloride, the title product described here.

2. Experimental

2.1. Preparations

The reactions were run under an argon atmosphere. The solvents were degassed and reagents used immediately after opening the phials.

2.1.1. $(Bu_4N)_2[Ni(C_2N_2S_{2.2}Se_{0.8})_2]$ (1)

$NaBH_4$ has been added slowly to powdered grey selenium (1.15 g, 14.6 mmol, 100 mesh, Aldrich reagent) dispersed in EtOH (15 ml) at 0 °C [11] until the solution cleared up (approximately 1.24 g, 32.8 mmol were required). The reagents were allowed to react under stirring until room temperature was reached. Then, NaOH (1.15 g, 29.0 mmol) in EtOH (20 ml) and successively $TDACl_2$ (2.75 g, 18.0 mmol) in EtOH (15 ml) have been added dropwise to the reaction mixture. The colour of the solution became brown. Bu_4NBr (1.61 g, 5.0 mmol) in EtOH (10 ml) and $NiCl_2 \cdot 6H_2O$ (0.60 g, 2.5 mmol) in the same solvent (20 ml) were added. A dark-brown solid precipitated immediately. This solid was removed by filtration (it was unsoluble in most common organic and inorganic solvents) and the filtered solution has been roto-evaporated. The obtained solid was dissolved in $(CH_3)_2CO$, giving a white residue and a yellowish-brown solution. Slow evaporation at room temperature of this solution gave yellowish-green crystals and a light yellow powder, which is suspended in diethyl ether (Et_2O) and removed from crystals. The crystals have been recrystallised from $(CH_3)_2CO/Et_2O$ at low temperature (−18 °C), giving rise to well-formed prismatic olive-green crystals of complex **1** (220 mg, yield ~10% based on nickel salt). Anal. Calc. for $C_{36}H_{72}N_6NiS_{4.4}Se_{1.6}$: C, 47.25; H, 7.93; N, 9.18; S, 15.42. Found: C, 46.98; H, 8.41; N, 9.22; S, 15.38%. IR [KBr pellets, cm^{-1}]: 2965s; 2940ms; 2880ms; 2210vw; 1490ms; 1475ms; 1460ms; 1405w; 1385ms; 1360vw; 1350vw; 1320ms; 1311s; 1230m; 1215vs; 1175w; 1150w; 1110w; 1080w; 1055w; 1030w; 1000w; 870m; 800w; 780m; 770s; 745mw; 720w; 490m; 435w. Raman (cm^{-1}): 2987mw; 2929m; 2868mw; 1441w; 1401vw; 1311s; 1185w; 1146vs; 762w; 380w; 284vw; 261w; 242w; 173s. UV–Vis [in $(CH_3)_2CO$], λ (nm) (ε, dm^3 mol^{-1} cm^{-1}): 394 sh; 454 (10 200).

2.1.2. $Bu_4N[Ni(C_2N_2S_{2.2}Se_{0.8})_2]$ (2)

I_2 (6.7 mg, 2.6×10^{-2} mmol) in acetone (10 ml) was slowly added to $(Bu_4N)_2[Ni(C_2N_2S_{2.2}Se_{0.8})_2]$ (48 mg, 5.2×10^{-2} mmol) in the same solvent (15 ml). The solution turned to green and was left 10 min under reflux. Crystals were obtained by slow diffusion of Et_2O into this solution (19.6 mg). Anal. Calc. for $C_{20}H_{36}N_5NiS_{4.4}Se_{1.6}$: C, 35.71; H, 5.39; N, 10.41; S, 20.97. Found: C, 35.88; H, 5.56; N, 10.32; S, 19.74%. IR [KBr pellets, cm^{-1}]: 2960ms; 2935m; 2878m; 1470s; 1445ms; 1405w; 1382ms; 1360vw; 1311ms; 1290w; 1235s; 1225vs; 1170w; 1125vw; 1110vw; 1085mw; 1065vw; 1030vw; 995vw; 920vw; 895mw; 880mw; 795ms; 780s; 770s; 740mw; 720w; 500m; 490m; 432w; 345mw. UV–Vis [in $(CH_3)_2CO$], λ (nm): 395; 445 sh; 466 sh; 804 sh; 920.

2.2. Measurements

Microanalyses were performed on a Carlo Erba CHNS elemental analyser model EA1108. IR spectra (4000–200 cm^{-1}) were recorded on KBr pellets with a Perkin–Elmer mod. 983 spectrometer. FT-Raman spectra (resolution: 4 cm^{-1}) were recorded on a Bruker RFS100 FT-spectrometer, fitted with an Indium–Gallium–Arsenide detector (room temperature) and operating with an excitation frequency of 1064 nm (Nd:YAG laser). The power level of the laser source varied between 20 and 40 mW. The solid samples were introduced in a capillary tube and then fitted into the compartment designed for a 180° scattering geometry. Electronic spectra (1500–300 nm) were recorded on a Cary 5 spectrophotometer. Cyclic voltammograms were carried out on an EG&G (Princeton Applied Research) potentiostat–galvanostat model 273, using a conventional three-electrode cell consisting of a platinum wire working electrode, a platinum wire as counterelectrode and Ag/AgCl in saturated KCl solution as reference electrode. The experiments were performed at room temperature (25 °C), in dry and argon-degassed CH_3CN containing 0.1 mol dm^{-3} Bu_4NPF_6 as supporting electrolyte, at 50–200 mV s^{-1} scan rate. Half-wave potential for ferrocene/ferrocenium couple (internal standard) is 0.43 V under the above conditions.

ESR spectra were carried out at room temperature on polycrystalline sample and in CH_2Cl_2 solution, using a Brücker 300 spectrometer at LCC-CNRS, Toulouse.

2.3. X-ray crystallography

A summary of data collection and structure refinement is reported in Table 1. Single crystal data were collected with an Enraf-Nonius CAD4 diffractometer (Cu Kα; $\lambda = 1.541838$ Å) for $(Bu_4N)_2[Ni(C_2N_2S_{2.2}Se_{0.8})_2]$ (**1**). Empirical absorption correction was applied using the program XABS2 [12]. This structure was solved by direct methods (SIR97) [13] and refined with full-matrix least-squares (SHELXL-97) [14], using the WINGX software package [15]. Non-hydrogen atoms were refined anisotropically. Coordinated sulfur and selenium (S1/Se1; S2/Se2) atoms were refined with the same positional and anisotropic parameters. The best result was obtained refining the structure with a site occupancy factor (s.o.f.) of 0.6 and 0.4, respectively. Se/S ratio: the refinement of the structure was carried out with a free refinement of the s.o.f. S/Se in the dithiolene core starting from the initial value of 0.5/0.5. Refinement s.o.f. S = 0.5, Se = 0.5 (around the Ni); Goodness-of-fit on $F^2 = 1.022$; Final R indices [$I > 2\sigma(I)$], $R_1 = 0.0496$, $wR_2 = 0.1630$; R indices (all data), $R_1 = 0.0663$, $wR_2 = 0.1630$. Refinement s.o.f. S = 0.6, Se = 0.4; Goodness-of-fit on $F^2 = 0.982$; Final R indices [$I > 2\sigma(I)$], $R_1 = 0.0430$, $wR_2 = 0.1208$; R indices (all data), $R_1 = 0.0590$, $wR_2 = 0.1328$.]

Table 1
Summary of crystallographic data for $(Bu_4N)_2[Ni(C_2N_2S_{2.2}Se_{0.8})_2]$

	(**1**)
Empirical formula	$C_{36}H_{72}N_6NiS_{4.4}Se_{1.6}$
Formula weight	915.11
Colour, habit	brown, block
Crystal size (mm)	0.38 × 0.36 × 0.36
Crystal system	monoclinic
Space group	$P2_1/n$
a (Å)	9.851(1)
b (Å)	15.973(2)
c (Å)	14.731(1)
β (°)	94.350(2)
V (Å^3)	2311.2(4)
Z	2
T (K)	293(2)
λ (Å)	1.541838
ρ_{calc} (Mg m^{-3})	1.315
μ (mm^{-1})	4.132
θ range (°)	4.09–69.99
No. of reflections/observed [$F > 4\sigma(F)$]	4335/3087
R_1	0.0430
wR_2	0.1208

$R_1 = \Sigma||F_o| - |F_c||/\Sigma|F_o|$, $wR_2 = \{\Sigma[w(F_o^2 - F_c^2)2]/\Sigma[w(F_o^2)^2]\}^{1/2}$, $w = 1/[\sigma^2(F_o^2) + (aP)^2 + bP]$, where $P = [\max(F_o^2, 0) + 2F_c^2]/3$.

Hydrogen atoms were placed at their calculated positions. The maximum and minimum peaks on the final difference Fourier map corresponded to 0.387 and −0.365 e Å^{-3}. The program PARST [16,17] was also used for an accurate analysis of the structure (presence of hydrogen bonds, least-square planes/lines, etc.). Full tables of bond lengths and angles, atomic positional parameters, anisotropic displacement parameters are given in the supplementary material.

3. Results and discussion

With the aim to obtain nickel complexes of 1,2,5-thiadiazole-3,4-diselenolate, the selenation of $TDACl_2$ has been attempted by using Na_2Se prepared in situ (Se/$NaBH_4$ in EtOH, as described in Section 2) and then adding nickel dichloride in the presence of Bu_4NBr and under an argon atmosphere. The olive-green $(Bu_4N)_2[Ni(C_2N_2S_{2.2}Se_{0.8})_2]$ (**1**) salt has been isolated and characterised. Structural data (see below) show that only a partial selenation reaction occurs and unexpectedly also sulfur atoms are present giving a mixed $Se_{0.4}/S_{0.6}$ occupancy of the thiolic sites in the anion. The presence of thiolic sulfur atoms in **1** and its low yield are ascribable to $TDACl_2$ ring opening for nucleophilic attack by hydride ions present in the reaction mixture. The formation of the intermediate **I** is proposed. This

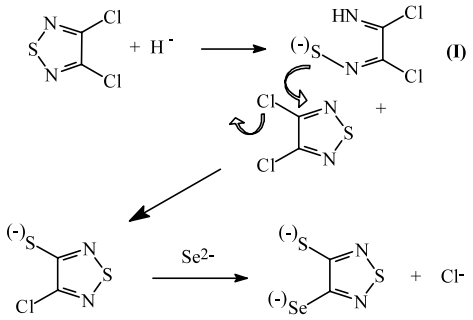

Scheme 1.

intermediate may follow decomposition pathways as well as it may react with $TDACl_2$ to form the dianion (see Scheme 1) which reacting with nickel ion produces **1**. To obtain reproducible results, unaged reagents and degassed solvents under argon atmosphere were used. More selective selenation methods are under investigation.

A crystal of **1** has been structurally characterised and the crystallographic data are summarised in Table 1. Similar to the $(Bu_4N)_2[Ni(tdas)_2]$ case, the crystal structure of **1** consists of dianionic complexes which occupy centrosymmetric positions (Fig. 1) and the cations fill holes between the anions. In the dianion, the central Ni-atom shows a square-planar geometry, as shown in Fig. 2. Table 2 lists the relevant bond distances and angles, and they are in agreement with those which are present in the tdas anion of the tetraethyl- and tetrabutyl-amonium salts. Ni–S/Se distances are close while the C–C length [1.428(5) Å] is significantly longer with respect to those found in $(Bu_4N)_2[Ni(C_3S_{2.5}Se_{2.5})_2]$ [d(Ni–S/Se) = 2.229(3), 2.245(1) Å; [d(C–C) = 1.32(2) Å] where a mixed $Se_{0.5}/S_{0.5}$ occupancy is found [18]. The C–C distance is close to the value [1.439(6) Å] found for $(Et_4N)_2[Ni(tdas)_2]$ [4b] and these values suggest a bond order significantly lower than two in tdas-based dianions.

The cyclic voltammogram of **1** is shown in Fig. 3, where one mono-electronic quasi-reversible oxidation at +0.13 V, one irreversible oxidation at approximately

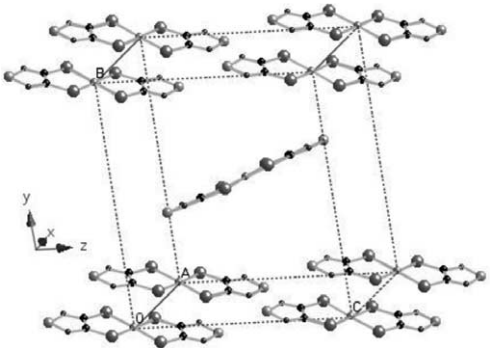

Fig. 1. Perspective view of the unit cell of $(Bu_4N)_2[Ni(C_2N_2S_{2.2}Se_{0.8})_2]$ (**1**), the Bu_4N cations are omitted for clarity.

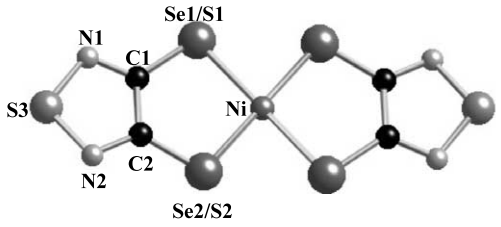

Fig. 2. Molecular structure of the anion $[Ni(C_2N_2S_{2.2}Se_{0.8})_2]^{2-}$ in **1**.

Table 2
Bond lengths (Å) and angles (°) for $[Ni(C_2N_2S_{2.2}Se_{0.8})_2]^{2-}$ with esd's [a]

C(1)–N(1)	1.324(4)	N(1)–C(1)–C(2)	114.2(3)
C(1)–C(2)	1.428(5)	N(1)–C(1)–Z(1)	123.6(3)
C(1)–Z(1)	1.798(3)	C(2)–C(1)–Z(1)	122.2(2)
C(2)–N(2)	1.317(4)	N(2)–C(2)–C(1)	113.1(3)
C(2)–Z(2)	1.796(3)	N(2)–C(2)–Z(2)	125.6(3)
N(1)–S(3)	1.659(3)	C(1)–C(2)–Z(2)	121.3(2)
N(2)–S(3)	1.633(4)	C(1)–N(1)–S(3)	106.5(3)
Ni–Z(2)	2.2565(5)	C(2)–N(2)–S(3)	108.2(3)
Ni–Z(1)	2.2844(6)	N(2)–S(3)–N(1)	98.1(2)
		C(1)–Z(1)–Ni	100.6(1)
		C(2)–Z(2)–Ni	101.7(1)
		Z(2)–Ni–Z(1)	93.90(2)
		Z(2) [b]–Ni–Z(1)	86.10(2)

[a] The dummy atom Z corresponds to S (s.o.f. = 0.6) and Se (s.o.f. = 0.4) for each coordination position.

[b] Symmetry transformations used to generate equivalent atoms: $-x+1$, $-y+1$, and $-z+1$.

0.67 V and one irreversible reduction at −0.39 V can be seen. The comparison of these results with the revised cyclic voltammetry data of the $(Bu_4N)_2[Ni(tdas)_2]$ complex (in the same +1.2 to −0.8 V range, Ag/AgCl in CH_3CN solution at 100 mV s^{-1} scan rate) ([8] and this work) shows that cyclic voltammetries are similar, but the oxidation processes are found respectively at $E_{1/2}$ = +0.18 V, E_a = +0.80 V; and a reduction wave is found

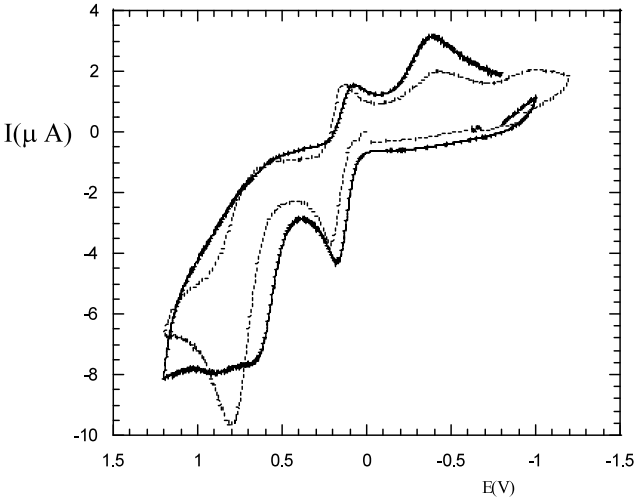

Fig. 3. Cyclic voltammetry of $(Bu_4N)_2[Ni(C_2N_2S_{2.2}Se_{0.8})_2]$ (—) and $(Bu_4N)_2[Ni(tdas)_2]$ (···) for comparison.

at $E_c = -0.42$ V, suggesting that the partial substitution of the thiolic sulfur with the selenium atoms makes easier the oxidation processes. Moreover the presence of the quasi-reversible wave at $E_{1/2} = +0.131$ V related to the process:

$$[Ni(C_2N_2S_{2.2}Se_{0.8})_2]^{2-} \underset{1\ \text{electron}}{\rightleftharpoons} [Ni(C_2N_2S_{2.2}Se_{0.8})_2]^{-}$$

suggests that the open-shell mono-anionic derivative containing Se-atoms is easily achievable and this complex seems suitable to be used as magnetic counterion of donors potential carriers of electro-conducting properties.

By chemical oxidation with I_2, a solid with analytical results in agreement with $Bu_4N[Ni(C_2N_2S_{2.2}Se_{0.8})_2]$ (**2**) has been obtained. The electronic spectrum of **2** shows the presence of a strong broad absorption in the near-infrared region at 920 nm in $(CH_3)_2CO$. This feature is typical of mono-anionic square-planar nickel dithiolene complexes [3].

In CH_2Cl_2 solution, an EPR signal with $g = 2.164$ is observed in agreement with the existence of the mono-anion as isolated species (Fig. 4). Solid samples of **2** do not give EPR signals suggesting that the monoanions with a delocalised electron form dimers strongly antiferromagnetically coupled, similarly to what happens in $(Bu_4P)_2[Ni(tdas)_2]$, where one sulfur atom of one ligands in a monoanion interacts with the nickel atom of another anion forming dimers [4c].

Vibrational spectroscopy has been successfully used to correlate the charge of square-planar metal dithiolene complexes with the position of the C=C stretch. This has been applied in the maleonitriledithiolate (mnt) complexes, where an infrared peak is found at 1485 cm^{-1} for the doubly negatively charged complexes $[M(mnt)_2]^{2-}$ and a peak at 1435 cm^{-1} for $[M(mnt)_2]^{-}$ [19]. More recent Raman studies refer to the $[M(dddt)_2]^{x-}$ case ($dddt^{n-} = 5,6$-dihydro-1,4-dithiin-2,3-dithiolate, $n = 0.6$, 2; M = Ni, Au, Pd, Pt, ν(C=C) in the 1300–1526 cm^{-1} range) [20] and $[M(dmit)_2]^{x-}$ ($x = 0$, 0.29, 0.5, 1, 2; M = Ni, Pd, ν(C=C) in the 1330–1435 cm^{-1} range) [21] series, where a linear correlation between this stretching vibration and the charge of the complexes have been found. This is explained considering that the C=C bond region of the ligands is bonding and gives a significant contribution to the HOMO (a π-orbital) of the negatively charged complexes. A C–C distance decrease is expected consequently but regular trends are not generally found (this has been explained taking into account mainly differences in crystal environment and accuracy of the structures) [22]. Surprisingly the vibrational spectra of **1** (IR and Raman) and **2** (IR) show a peak which may be assigned to the C=C stretching vibration at 1311 cm^{-1}. To support this, Raman spectra on $(Bu_4N)_2[Ni(tdas)_2]$ of $(Bu_4N)[Ni(tdas)_2]$ complexes, both structurally characterised, have been run (see Fig. 5). The comparison of the Raman spectra of $(Bu_4N)_2[Ni(tdas)_2]$ and $(Bu_4N)_2[Ni(C_2N_2S_{2.2}Se_{0.8})_2]$ is reported in Fig. 6. As it can be observed the spectra are very similar, and the main difference is due to the disappearance in (**1**) of Ni–S stretching, which appears at 386 cm^{-1} in $(Bu_4N)_2[Ni(tdas)_2]$. The position of the ν(C=C) peak which does not undergo a significant shift with the charge (−1, −2), suggests that the contribution of the p_z orbitals of the carbon atoms to the HOMO, should be significantly lower that in the corresponding mnt, dddt and dmit derivatives. Approximate theoretical calculations on $[Ni(tdas)_2]^{2-}$ and on the corresponding $[Ni(tdase)_2]^{2-}$ diselenole complex based on approximate Extended Huckel methods, by using the CACAO program [23] have been performed. The contributions of the p_z AO are as follows: terminal sulfur (18%), carbon (8%), nitrogen (4%), inner sulfur (15%) atoms for each ligand and nickel (d_{xz} 10%) to the HOMO (in agreement with the values reported in Ref. [8]). Similarly for the

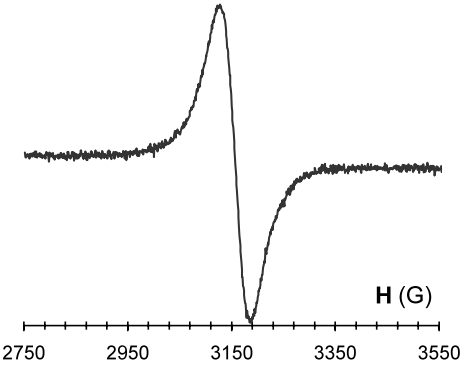

Fig. 4. The EPR spectrum of $Bu_4N[Ni(C_2N_2S_{2.2}Se_{0.8})_2]$ (**2**) in CH_2Cl_2 solution at room temperature ($G = 10^{-4}$ T).

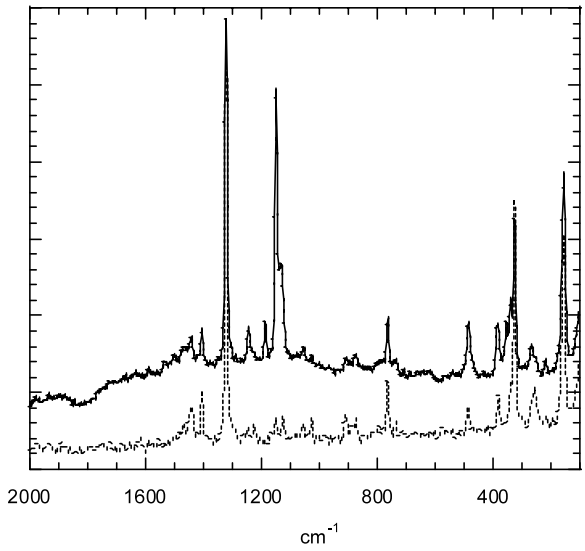

Fig. 5. Raman spectra $(Bu_4N)_2[Ni(tdas)_2]$ (—) and $(Bu_4N)[Ni(tdas)_2]$ (···) for comparison.

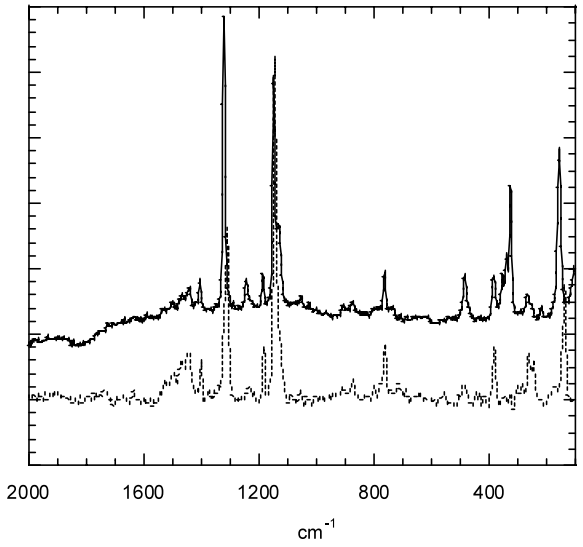

Fig. 6. Raman spectra $(Bu_4N)_2[Ni(tdas)_2]$ (—) and $(Bu_4N)_2[Ni(C_2N_2S_{2.2}Se_{0.8})_2]$ (···) for comparison.

corresponding diselenole complex the contributions are: HOMO, terminal selenium (12%), carbon (10%), nitrogen (6%), inner sulfur (18%) atoms for each ligand and nickel (d_{xz} 11%). In Fig. 7 the frontier orbitals for the $[Ni(tdase)_2]^{2-}$ anion are shown. It can be seen that the contribution of the sulfur/selenium atoms, prevails in the HOMO, and the bond region is delocalised over the N–C–C–N moiety. Consequently, the population of this orbital on going from −1 to −2 charged species should have a low influence on the C=C bond order. A higher contribution of the C=C bond region is found in the corresponding MO of the nickel dithiolenes cited above (see Ref. [20] for the dddt case and Refs. [24,25] for mnt and dmit, respectively). This can explain the difference in the trend of the ν(C=C) with the charge for the different complexes.

4. Conclusions

The new $(Bu_4N)_2[Ni(C_2N_2S_{2.2}Se_{0.8})_2]$ redox active nickel complex with a mixed $S_{0.6}/Se_{0.4}$ occupancy of thiolic sulfurs in the tdas ligand has been prepared and characterised, as well as its mono-oxidation product. Raman measurements have shown that in this case, as well as in tdas derivatives, no significant shift of the ν(C=C) with the charge is found, differently to what observed in metal dithiolene complexes based on dmit, mnt and dddt ligands. The introduction of the selenium atom in the dithiolene core has the effect to make the dianion more easier to oxidise than the corresponding tdas derivative. The dianionic and monoanionic species seem interesting to be used as diamagnetic and paramagnetic counterions of donors derived from ET, to prepare conducting molecular materials with the view to compare the role of these counterions as well as of the selenium atoms on the properties of the CT salts.

More effective selenation methods to achieve the seleno-isologs of tdas are in course.

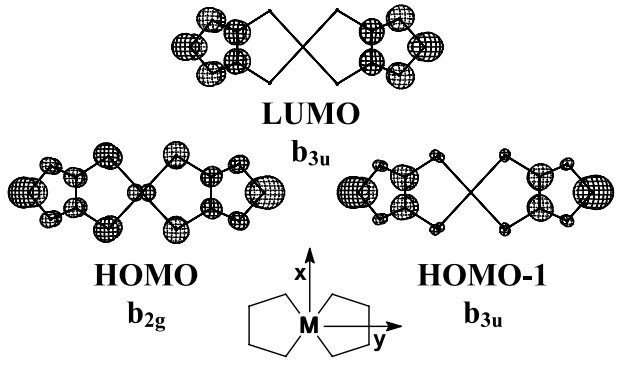

Fig. 7. Frontier MOs of $[Ni(tdase)_2]^{2-}$.

5. Supplementary material

Crystallographic data for the structural analyses have been deposited with the Cambridge Crystallographic Data Center, CCDC No. 195701 for compound **1**. Copies of this information may be obtained free of charge from The Director, CCDC, 12 Union Road, Cambridge, CB2 1EZ, UK (Fax: +44-1223-336033; e-mail: deposit@ccdc.cam.ac.uk or http://www.ccdc.cam.ac.uk).

Acknowledgements

This work has been developed in the framework of European COST action D14 "Towards New Molecular Inorganic Conductors". Thanks are due to Dr. Alain Mari and Equipe "Précurseurs Moléculaires et Matériaux" LCC-CNRS, Toulouse, France, for running EPR spectra.

References

[1] (a) P. Cassoux, L. Valade, in: D.W. Bruce, D. O'Hare (Eds.), Inorganic Materials, 2nd ed., Wiley, Chichester, 1996;
(b) H. Tanaka, Y. Okano, H. Kobayashi, W. Suzuki, A. Kobayashi, Science 291 (2001) 285.
[2] (a) A.T. Coomber, D. Beljonne, R.H. Friend, J.K. Brédas, A. Charlton, N. Robertson, A.E. Underhill, M. Kurmoo, P. Day, Nature 380 (1996) 144;
(b) N. Robertson, L. Cronin, Coord. Chem. Rev. 227 (2002) 93.
[3] (a) U.T. Mueller-Westerhoff, B. Vance, D.I. Yoon, Tetrahedron 47 (1991) 909;
(b) C.S. Winter, C.A.S. Hill, A.E. Underhill, Appl. Phys. Lett. 58 (1991) 107.
[4] (a) I. Hawkins, A.E. Underhill, J. Chem. Soc., Chem. Commun. (1990) 1593;
(b) O.A. Dyachenko, S.V. Konovalikhin, A.I. Kotov, G.V.

Shilov, E.B. Yagubskii, C. Faulmann, P. Cassoux, J. Chem. Soc., Chem. Commun. (1993) 508;
(c) S. Schenk, I. Hawkins, S.B. Wilkes, A.E. Underhill, A. Kobayashi, H. Kobayashi, J. Chem. Soc., Chem. Commun. (1993) 1648;
(d) G. Wolmershäuser, R. Johann, Angew. Chem., Int. Ed. Engl. 28 (1989) 920.
[5] M. Bousseau, L. Valade, J.P. Legros, P. Cassoux, M. Garbauskas, L.V. Interrante, J. Am. Chem. Soc. 108 (1986) 1908.
[6] K. Awaga, T. Okuno, Y. Maruyama, A. Kobayashi, H. Kobayashi, S. Schenk, A.E. Underhill, Inorg. Chem. 33 (1994) 5598.
[7] (a) N. Robertson, K. Awaga, S. Parsons, A. Kobayashi, A.E. Underhill, Adv. Mater. Opt. Electron. 8 (1998) 93;
(b) K. Awaga, J.D. Kilburn, N. Le Narvor, N. Robertson, A.E. Underhill, J. Ziegenbalg, Mol. Cryst. Liq. Cryst. 284 (1996) 39.
[8] H. Yamochi, N. Sogoshi, Y. Simizu, G. Saito, K. Matsumoto, J. Mater. Chem. 11 (2001) 2216.
[9] P. Deplano, L. Leoni, M.L. Mercuri, J.A. Schlueter, U. Geiser, H.H. Wang, A.M. Kini, J.L. Manson, C. Gomez-Garcia, E. Coronado, M.-H. Whangbo, J. Mater. Chem. 12 (2002) 3570.
[10] L. Pilia, C. Faulmann, I. Malfant, V. Collière, M.L. Mercuri, P. Deplano, P. Cassoux, Acta Crystallogr., Sect. C 58 (2002) 240.
[11] D.L. Klayman, T.S. Griffin, J. Am. Chem. Soc. 95 (1973) 197.
[12] S. Parkin, B. Moezzi, H. Hope, J. Appl. Crystallogr. 28 (1995) 53.
[13] A. Altomare, M.C. Burla, M. Camalli, G.L. Cascarano, C. Giacovazzo, A. Guagliardi, A.G.G. Moliterni, G. Polidori, R. Spagna, J. Appl. Crystallogr. 32 (1999) 115.
[14] G.M. Sheldrick, SHELX-97. Programs for Crystal Structure Analysis, University of Göttingen, Germany, 1997.
[15] L.J. Farrugia, J. Appl. Crystallogr. 32 (1999) 837.
[16] M. Nardelli, Comput. Chem. 7 (1983) 95.
[17] M. Nardelli, J. Appl. Crystallogr. 28 (1995) 659.
[18] G. Matsubayashi, S. Tanaka, A. Yokozawa, J. Chem. Soc., Dalton Trans. (1992) 1827.
[19] (a) C.W. Schläpfer, K. Nakamoto, Inorg. Chem. 14 (1975) 1338;
(b) J.L. Wootton, J.I. Zink, J. Phys. Chem. 99 (1995) 7251;
(c) S. Kutsumizu, N. Kojima, T. Ban, I. Tsujikawa, Bull. Chem. Soc. Jpn. 60 (1987) 2547.
[20] H.H. Wang, S.B. Fox, E.B. Yagubskii, L.A. Kushch, A.I. Kotov, M.-H. Whangbo, J. Am. Chem. Soc. 119 (1997) 7601.
[21] K.I. Pokhodnya, C. Faulmann, I. Malfant, R. Andreu-Solano, P. Cassoux, A. Mlayah, D. Smirnov, J. Leotin, Synth. Met. 103 (1999) 2016.
[22] B.S. Lim, D.V. Fomitchev, R.H. Holm, Inorg. Chem. 40 (2001) 4257.
[23] C. Mealli, D. Proserpio, J. Chem. Educ. 67 (1990) 39.
[24] A. Kobayashi, Y. Sasaki, Bull. Chem. Soc. Jpn. 50 (1977) 2650.
[25] M. Nakano, A. Kuroda, T. Maikawa, G.-E. Matsubayashi, Mol. Cryst. Liq. Cryst. 284 (1996) 301.